JCTC Journal of Chemical Theory and Computation

Article

pubs.acs.org/JCTC

Revisiting the Nonadiabatic Process in 1,2-Dioxetane

Pooria Farahani,[†] Daniel Roca-Sanjuán,*[,‡] Felipe Zapata,[§] and Roland Lindh*[,†]

[†]Department of Chemistry, Ångström, Uppsala University, P.O. Box 518, SE-751 20 Uppsala, Sweden

[‡]Instituto de Ciencia Molecular, Universitat de València, P.O. Box 22085, ES-46071 València, Spain

[§]Departamento de Quimica Fisica, Universidad de Alcalá, E-28871, Alcalá de Henares, Madrid, Spain

Supporting Information

ABSTRACT: Determining the ground and excited-state decomposition mechanisms of 1,2-dioxetane is essential to understand the chemiluminescence and bioluminescence phenomena. Several experimental and theoretical studies has been performed in the past without reaching a converged description. The reason is in part associated with the complex nonadiabatic process taking place along the reaction. The present study is an extension of a previous work (De Vico, L.; Liu, Y.-J.; Krogh, J. W.; Lindh, R. *J. Phys. Chem. A* **2007**, *111*, 8013−8019) in which a two-step mechanism was established for the chemiluminescence involving asynchronous O−O′ and C−C′ bond dissociations. New high-level multistate multi configurational reference second-order perturbation theory calculations and *ab initio* molecular dynamics simulations at constant temperature are performed in the present study, which provide further details on the mechanisms and allow to rationalize further experimental observations. In particular, the new results explain the high ratio of triplet to singlet dissociation products.

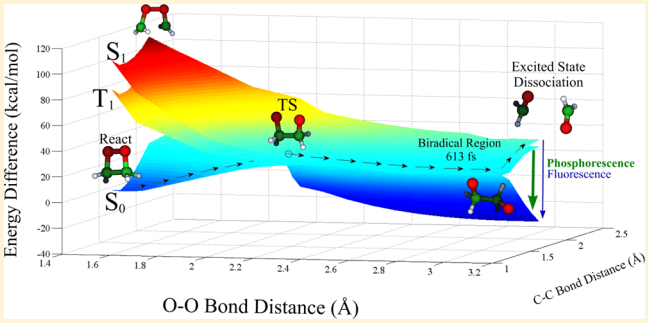

1. INTRODUCTION

The phenomenon that a chemical reaction generates a light emitting product is called chemiluminescence, the same phenomenon observed in living organisms is referred to as bioluminescence. The phenomenon is used as a practical tool in medicine and chemistry. This is easily seen in the large amount of biotechnological applications, for example, as a research tool in genetic engineering with the use of reporter genes,[1] or as a noninvasive study of biochemical processes in living small laboratory animals through bioluminescence imaging.[2] Nature provides us with plenty of examples of such phenomena, of which the firefly beetle is the most well-known. The bioluminescence is in principle a catalyzed version of chemiluminescence involving a substrate, luciferin, and an enzyme, luciferase, which will catalyze the chemical reaction. Oxidation of luciferins, yields a peroxy compound, called 1,2-dioxetane. This four-membered ring peroxide has been shown to be a common functional group in chemi- and bioluminescent systems. Accordingly, the thermal decomposition of isolated 1,2-dioxetane is the most simple example of the chemi- and bioluminescence reaction. A detailed description of the process in this system at the molecular level is key to an unified understanding of the chemistry of bioluminescence. During the last 20 years, significant theoretical and experimental efforts have been performed to understand the mechanism of the thermally activated chemi- and bioluminescence. According to these efforts, three different mechanisms have been proposed for the thermal dissociation of 1,2-dioxetane; the biradical, concerted, and merged mechanisms (see Figure 1). The biradical mechanism is a two-step reaction in which the C−C′ bond breaking occurs after the complete breakage of the O−O′ bond—the intermediate product has a biradical character. The concerted reaction is a single-step process in which the O−O′ and C−C′ bond breakage occur simultaneously. Finally, the merged mechanism implies that the C−C′ cleavage starts before the O−O′ bond breaking is fully completed. It is also well-known that three channels compete in the decomposition of 1,2-dioxetane giving rise to two formaldehyde fragments (see Figure 1). A small fraction of the formaldehyde molecules is generated in an excited state, from which the system returns to the ground state by emitting light. Both singlet and triplet paths are possible, thus producing fluorescence and phosphorescence emission, respectively. The remaining fraction of formaldehyde products is formed without emission of radiation.

Luminescence in thermal decomposition of 1,2-dioxetane systems, in particular, 3,3,4-trimethyl-1,2-dioxetane, was early (in 1968) observed by Kopecky and Mumford.[3] In this study, an emission of light associated with an activation energy of 25 kcal/mol was interpreted to be due to a singlet excited state in a concerted reaction. Next, in 1970, O'Neal and Richardson[4] hypothesized that 1,2-dioxetane decomposition should proceed similarly to analogous saturated four-membered ring systems, such as cyclobutane, whose thermochemical data clearly showed a two-step biradical mechanism. The authors demonstrated that the observed experimental kinetic data and

Received: September 3, 2013

   dx.doi.org/10.1021/ct4007844 | *J. Chem. Theory Comput.* XXXX, XXX, XXX−XXX

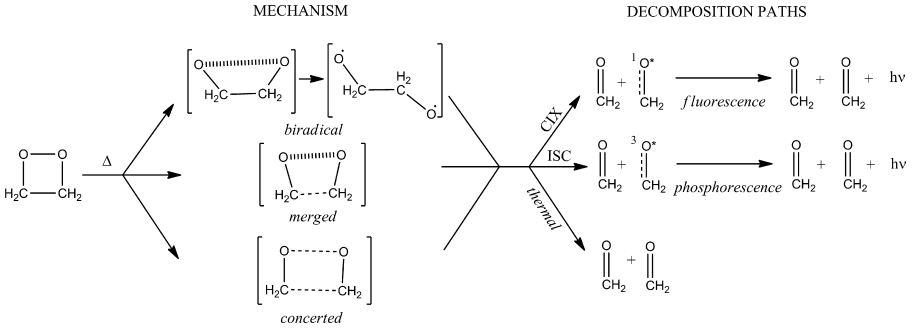

Figure 1. Mechanisms proposed in the literature and dissociation channels for the chemiluminescent reaction of 1,2-dioxetane.

the thermochemical calculations were consistent with such a mechanism.[4] A series of works appeared later introducing and giving support to the merged (or asynchronous concerted) mechanism on the basis of the highly efficient chemiexcitation found in methyl-substituted 1,2-dioxetanes, arguing that a biradical mechanism would result in the formation of basically only ground state products.[5,6] Adam and Baader[6] also reported in some of these studies that the thermal dissociation and chemiluminescence have the same activation energy and that phosphorescence in 1,2-dioxetane is favorable over fluorescence by a factor of 1000. In the 1990s, Olivucci, Robb, and co-workers[7,8] performed *ab initio* theoretical studies employing the complete active space self-consistent field (CASSCF) method with Möller−Plesset second-order perturbation theory (MP2) corrections to explore the potential energy surfaces (PESs) of the ground state and lowest-lying triplet excited state. The authors characterized the singlet−triplet crossing (ISC) regions that mediate the chemiexcitation process. A biradical region was also determined in the triplet energy surface between the transition states (TSs) related to O−O′ and C−C′ bond cleavage. These TS structures were found at similar energies, therefore supporting previous experimental findings from Adam and Baader[6] and other measurements for tetramethyldioxetane[9] and *cis*-diethoxy-1,2-dioxetane.[10] Nevertheless, Wilsey et al.[8] computed a value of 16 kcal/mol for the activation energy for the ring-opening of 1,2-dioxetane, which was clearly lower than the experimental observed value (22 kcal/mol).[6] In 2007, De Vico et al.[11] employed a higher level of theory using the multistate complete active space second-order perturbation theory (MS-CASPT2) method to study the dissociation process, finding a more accurate value for the activation energy of the thermal dissociation in agreement with the experiment.[6] De Vico et al. also studied the lowest-lying triplet excited states and considered in addition the lowest-lying singlet excited state which give rise to fluorescence. Conical intersections (CIX) and singlet−triplet ISC crossings were identified, and an entropic trapping of biradical character was obtained similarly to Wilsey et al.[8] The activation barriers for the O−O′ cleavage were obtained, however, at higher energies with respect to those related to the C−C′ bond breaking on the singlet and triplet excited states. Most recently, a direct dynamics simulation of the dissociation at the unrestricted density functional theory level of approximation has been carried out by Sun et al.[12] who have found on the ground state that some trajectories proceeded with an almost simultaneous O−O′ and C−C′ bond dissociations after the formation of 1,2-dioxetane.[12] They also found that the kinetics showed a strong non-RRKM behavior. To conclude, experimental and theoretical investigations are not conclusive with respect to the nature of the reaction mechanism, although there are evidence in support of biradical characteristics. While theory and experiment finally agree on the activation energy of the ground state dissociation process, details on the ratio of the phosphorescence and fluorescence emissions and the activation energy of the chemiluminescence are not correctly taken into account.

The aim of the present study is to clarify the qualitative concept and complete our previous quantitative study with additional results, which allow us to rationalize most of the experimental observations. In particular, we put some efforts in understanding the large ratio phosphorescence/fluorescence of the chemiluminescence emission, which was not explained on the basis of the results obtained from the previous study.[11] Electronic structure calculations using the CASSCF and MS-CASPT2 methods have been carried out in association with *ab initio* molecular dynamics (AIMD) at constant temperature (the canonical ensemble). The present study is subsequently structured as follows, a section with the computational details with regard to the electronic structure and *ab initio* molecular dynamics simulations, a section of presentation and discussion of the results, and finally some conclusions.

2. COMPUTATIONAL DETAILS

Details about the electronic structure and the AIMD computations are given below.

2.1. Electronic Structure. The CASSCF[13,14] and CASPT2[15−17] methods were employed for the geometry optimizations of the stationary points in conjunction with the atomic natural orbital (ANO-RCC)[18] basis set contracted to O,C[4s3p2d1f]/H[3s2p1d] (hereafter ANO-RCC-VTZP). Additional CASPT2 energy computations were performed at the CASSCF and CASPT2 geometries improving the basis set from triple-ζ to quadruple-ζ quality, in particular, using the ANO-RCC[18] basis set contracted to O,C[5s4p3d2f1g]/H[4s3p2d1f] (hereafter ANO-RCC-VQZP). The same active space as the one employed in the previous study was used, that is, 12 electrons distributed in 10 orbitals.[11] It corresponds to the C−C′, C−O, C′−O′, and O−O′ σ bonding and σ^* antibonding orbitals plus the two oxygen lone-pair orbitals (n_O). To account for all the degenerate combinations of the electrons in the oxygen (n_O) orbitals in the biradical region of the chemiluminescence mechanism (see Figure 2), four equally weighted roots were employed in the state averaged (SA) CASSCF procedure for all the CASSCF computations. Energies of the lowest-lying four singlet (S_0, S_1, S_2, and S_3) and four triplet (T_1, T_2, T_3, and T_4) states were calculated. Zero-point vibrational energy (ZPVE) corrections were computed numerically at the SA(4)-CASSCF/ANO-RCC-VQZP level through the second-order derivatives of the energy using the harmonic

dx.doi.org/10.1021/ct4007844 | J. Chem. Theory Comput. XXXX, XXX, XXX−XXX

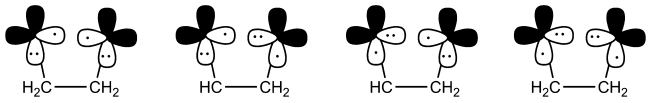

Figure 2. Electron occupation of the oxygen lone-pair orbitals at the biradical region of the chemiluminescence and thermal mechanisms of 1,2-dioxetane.

approximation. The multistate (MS) approach[19] of the CASPT2 method was used throughout to keep the consistency with the previous work.[11] Unless stated otherwise, the CASPT2 results shown in this paper are MS-CASPT2 results. The state specific (SS) CASPT2 and MS-CASPT2 methods give rise to energy values with deviations lower than 1 kcal/mol (see Supporting Information Table S2). The MS and SS approaches were compared along the extended region of state crossing, verifying that the out-of-diagonal elements of the effective Hamiltonian defined in the MS approach are in all the cases lower than 2−3 kcal/mol, which point to an accurate characterization of the mechanism with the MS-CASPT2 method.[20] As for the previous work,[11] core orbitals of non-hydrogen atoms were frozen in all the MS-CASPT2 calculations and the standard ionization potential electron affinity (IPEA) modification of the zeroth-order Hamiltonian with a value of 0.25 was employed.[21]

The energy profiles relevant for the chemiluminescence mechanism of 1,2-dioxetane were mapped at the MS-CASPT2//CASSCF(12in10)/ANO-RCC-VTZP level by means of the constrained optimization technique, using the C−C′ and O−O′ bond distances as constraints.[22] In each calculation, these bond distances were kept fixed and all the other internal coordinates were optimized. The range of values for the C−C′ and O−O′ bond lengths are 1.42−2.02 and 1.48−3.08 Å, respectively, with a step size of 0.1 Å. Other possibilities were also considered for the constraints. In particular, the C−C′ bond distance plus the O−C−C′−O′ dihedral angle. In this case, the former internal coordinate ranges also 1.42−2.02 Å, with a step size of 0.1 Å, and the values for the dihedral angle are between 0° and 180°, with different step sizes.

Spin−orbit coupling (SOC) terms between singlet and triplet states were computed within the AMFI and CASSI frameworks,[23,24] as implemented in the MOLCAS-7 quantum-chemistry program.[25] A CASSCF(12in10)/ANO-RCC-VQZP wave function averaged over four singlet and four triplet states was used.

2.2. *Ab Initio* Molecular Dynamics. The standard formulation of the molecular dynamics results in trajectories belonging to the microcanonical (NVE) ensemble. In this ensemble, the number of particles, volume, and total energy of the system is preserved. Nevertheless, most of the chemical experiments are carried out at constant temperature, the statistical behavior of which is described by the canonical (NVT) ensemble. An approach to take into account the temperature is the Nosé-Hoover chain of thermostats, in which the molecular system is coupled to a heat bath, generating the correct canonical ensemble.[26]

Therefore, improvements to the MOLCAS package were introduced to facilitate molecular dynamics simulations in the canonical ensemble, through the Nosé-Hoover method, which permits to include in the Hamiltonian the required degrees of freedom to simulate a thermostat.[27] The resulting motion equations were integrated by a time reversible integrator, applying the Liouville approach through the Trotter factorization.[28] The chosen initial conditions assumed that the particles velocities obey the Maxwell−Boltzmann distribution, therefore every component of the velocity can be considered as an independent Gaussian random variable for a given temperature.[29]

The methodology of the molecular dynamics at a constant temperature of 300 K was applied to the 1,2-dioxetane molecule for simulating the dynamical behavior in the so-called entropic trapping volume of the phase space. "On-the-fly" molecular dynamics were performed on S_0, starting from the TS of the thermal decomposition (TS_{S0}). By initiating the dynamics trajectories at the TS, the efficiency of the dynamics simulations is enhanced since the proper vibrational modes are enforced. Previous studies have also employed this approach,[12,30,31] showing that TS sampling gives dynamics results in agreement with experiments under the transition state theory (TST) approximation.[30,31] A set of 300 trajectories were run with an integration step of 1 fs and a maximum simulation time of 4 ps. The molecule was considered out of the biradical region when the distance between the carbon atoms of the two formaldehyde moieties was larger than 2.3 Å.

To perform the dynamics simulations, we tested in advance less time-demanding CASSCF/CASPT2 approaches than those mentioned in the previous section. The basis set and active space that maximize the ratio accuracy/time are the double-ζ quality ANO-RCC basis set contracted to O,C[3s2p1d]/H[2s1p] (hereafter, ANO-RCC-VDZP) and 8 electrons distributed in 6 orbitals, respectively. Since the C−O and C′−O′ bonds do not break in the chemiluminescence mechanism, the occupation numbers of the σ and σ^* orbitals of the C−O and C′−O′ orbitals are very close to two and zero, respectively. Hence, the results are still accurate enough when these four orbitals are removed from the active space. The MS-CASPT2 energies of the lowest-lying four singlet and four triplet states were computed at each integration step. These values were also employed together with the C−C′ distance to evaluate the departure of the molecule from the entropic-trapping region.

A development version of the MOLCAS-7 quantum-chemistry package suite was used in all electronic structure and molecular dynamics simulations of this study.[25]

3. RESULTS AND DISCUSSION

The findings obtained for the chemiluminescence mechanism of 1,2-dioxetane are presented in three sections. First, the analysis of the geometries and energies is presented for the stationary points obtained with the different CASSCF/CASPT2 approaches. Next, the details of the mechanism are explained using a two-dimensional model of the PESs for the lowest-lying four singlet and four triplet states. Finally, a few dynamical properties of the dissociation reaction are discussed.

3.1. Stationary Points of the Thermal and Chemiluminescence Mechanism. Several structures were found in the previous work by De Vico et al.,[11] which are relevant for the mechanism of thermally activated light emission of the 1,2-dioxetane molecule: the starting geometry (Reactant), the TS involving O−O′ bond breaking (TS_{S0}), the singlet and triplet biradical minima with O−C−C′−O′ dihedral angles of 70° ($Min_{S1(70)}$ and $Min_{T1(70)}$) and 180° ($Min_{S1(180)}$ and $Min_{T1(180)}$), the singlet and triplet TS involving C−C′ bond breaking with dihedral angle 70° ($TS_{S1(70)}$ and $TS_{T1(70)}$) and 180° ($TS_{S1(180)}$ and $TS_{T1(180)}$), and the products on the excited singlet [OCH_2

dx.doi.org/10.1021/ct4007844 | J. Chem. Theory Comput. XXXX, XXX, XXX−XXX

+ $^1(OCH_2)$] and triplet states [OCH_2 + $^3(OCH_2)$]. Note that in this work we have used a slightly different notation, the type A and B TSs of De Vico et al.[11] are those that we denote 70 and 180, respectively, although the actual angles are not exactly 70 and 180°. Note also that the TSs at the dihedral angle of 70° have a symmetry partner at −70°.

In this work, CASSCF(12in10)/ANO-RCC-VTZP geometries from De Vico et al.[11] were reoptimized, and subsequently, MS-CASPT2 geometry optimizations with the same active space and basis set were carried out. Table 1 compiles the computed C−C′ and O−O′ bond distances and the O−C−C′−O′ dihedral angle (see Cartesian coordinates in Table S1). The CASSCF and MS-CASPT2 results show small differences for all the internal coordinates of the bound structures, with average deviations of 0.05 Å, 0.06 Å, and 2° for the O−O′ and C−C′ bonds and the O−C−C′−O′ dihedral angle, respectively. As expected from the lower accuracy of the CASSCF method to describe noncovalent interactions, the largest deviations appear for the complex formed between the two formaldehyde molecules once the O−O′ and C−C′ bond dissociations take place. Overall, the CASSCF method is accurate enough for the geometry optimization of the 1,2-dioxetane and all the intermediates in the chemiluminescence mechanism. However, energy values are dramatically affected by the dynamical correlation. This fact is observed, for example, at the TS_{S0} structure, in which the CASSCF method underestimates the activation energy for O−O′ bond breaking by 14.0 kcal/mol (see Table 2). Much lower deviations occur in the comparison of the MS-CASPT2/ANO-RCC-VTZP energies obtained at the CASSCF/ANO-RCC-VTZP or MS-CASPT2/ANO-RCC-VTZP geometries, with an average difference of 1.8 kcal/mol.

Next, in order to analyze the basis set effect on the energies, we performed calculations with the ANO-RCC-VQZP basis set at the CASSCF/ANO-RCC-VTZP and MS-CASPT2/ANO-RCC-VTZP optimized geometries. Large discrepancies appear in the case of the vertical excitation energies between the four singlet and four triplet states computed (see Supporting Information Table S2). Conversely, the relative energies between the stationary structures are much less affected, showing average deviations of 1.3 and 2.8 kcal/mol at the CASSCF/ANO-RCC-VTZP and MS-CASPT2/ANO-RCC-VTZP geometries, respectively (cf. Table 2). In all the points along the mechanism, the ANO-RCC-VQZP basis set gives rise to larger energy values relative to the reactant, being the $TS_{(180)}$ structures the most sensitive. It is worth noting that almost no differences are found with the larger basis set between the energies obtained at the CASSCF and MS-CASPT2 geometries (average deviation of 0.3 kcal/mol, always lower than 1.4 kcal/mol).

Further improvements to the mechanism come from the inclusion of ZPVE corrections (see Table 3). Since the presence of four roots in the SA procedure within the CASSCF method is needed to describe properly the geometries and energetics in the biradical region, the second-order derivatives of the energy were computed numerically at the CASSCF(12in10)/ANO-RCC-VTZP level. The entropic factor was also estimated by means of these calculations. The ZPVE results show a clear pattern: each bond dissociation implies a decrease of around 2 kcal/mol in the values of the corresponding TS. Thus, taking into account the ZPVE corrections, the TS_{S0}

Table 1. Main Geometrical Parameters of 1,2-Dioxetane Optimized at the CASSCF/ANO-RCC-VTZP (left) and MS-CASPT2/ANO-RCC-VTZP (right) Levels of Theory[a]

	C−C′	O−O′	O−C−C′−O′
react	1.51/1.49	1.58/1.51	17/19
TS_{S0}	1.54/1.49	2.26/2.28	37/44
$Min_{T1(70)}$	1.55/1.51	3.11/3.02	77/77
$Min_{S1(70)}$	1.53/1.53	2.98/2.92	66/75
$Min_{T1(180)}$	1.55/1.51	3.68/3.60	180/179
$Min_{S1(180)}$	1.55/1.54	3.70/3.54	180/179
$TS_{T1(70)}$	2.02/2.07	3.27/3.25	79/83
$TS_{S1(70)}$	2.09/2.21	3.27/3.25	76/76
$TS_{T1(180)}$	2.02/2.08	3.76/3.73	180/180
$TS_{S1(180)}$	2.08/2.19	3.81/3.82	180/180
$Prod_{T1}$	4.47/3.45	4.63/3.61	156/179
$Prod_{S1}$	4.15/3.41	4.06/3.57	136/180

[a]Bond lengths in Å and dihedral angles in degree.

Table 2. Relative Energies (in kcal/mol) of the Main Stationary Structures of 1,2-Dioxetane in the Chemiluminescence Mechanism Computed with Different CASSCF/CASPT2 Approaches[a]

	CASSCF/TZ	MS-CASPT2//CASSCF/TZ	MS-CASPT2/TZ	MS-CASPT2/QZ//CASSCF/TZ	MS-CASPT2/QZ//MS-CASPT2/TZ
react	0.0	0.0	0.0	0.0	0.0
TS_{S0}	9.7	23.7	23.4	24.9	25.5
$Min_{T1(70)}$	7.7	18.4	17.8	19.6	20.0
$Min_{S1(70)}$	9.0	18.4	17.2	19.6	19.4
$Min_{T1(180)}$	7.1	17.9	18.5	19.1	19.9
$Min_{S1(180)}$	8.8	18.1	16.6	19.2	18.7
$TS_{T1(70)}$	22.2	30.0	28.4	31.7	31.2
$TS_{S1(70)}$	26.5	35.0	33.7	36.6	36.3
$TS_{T1(180)}$	21.1	29.0	24.2	30.6	30.4
$TS_{S1(180)}$	25.7	34.3	29.4	35.9	35.6
$Prod_{T1}$	7.2	25.3	22.1	27.0	25.5
$Prod_{S1}$	13.2	32.4	29.5	34.1	32.7

[a]Vertical excitation energies for the other singlet and triplet states at these geometries are compiled in Table S2.

Table 3. Zero-Point Vibrational Energy Corrections and Gibbs Energies (in kcal/mol) at 300 K of the Main Stationary Structures of 1,2-Dioxetane in the Chemiluminescence Mechanism Computed at the CASSCF/ANO-RCC-VTZP Level of Theory

	ZPVE	Gibbs energy
react	40.2	23.9
TS_{S0}	38.4	21.8
$Min_{T1(70)}$	38.1	21.2
$Min_{S1(70)}$	37.0	20.2
$Min_{T1(180)}$	38.2	21.3
$Min_{S1(180)}$	37.5	20.6
$TS_{T1(70)}$	35.0	17.6
$TS_{S1(70)}$	36.0	18.5
$TS_{T1(180)}$	35.9	18.7
$TS_{S1(180)}$	35.5	18.1
$Prod_{T1}$	33.7	14.0
$Prod_{S1}$	34.0	13.1

dx.doi.org/10.1021/ct4007844 | J. Chem. Theory Comput. XXXX, XXX, XXX−XXX

structure is stabilized by 1.8 kcal/mol with respect to the reactant, and the energies of the $TS_{(70)}$ and $TS_{(180)}$ on the singlet and triplet manifolds decrease an average of 4.8 and 4.5 kcal/mol, respectively, also with respect to the close-ring dioxetane. Bond dissociation also changes the entropy of the molecule along the mechanism, stabilizing further the opened structures. Our results show a decrease of 2.1 kcal/mol for the TS_{S0} structure and an average decrease of 5.9 and 5.5 kcal/mol for the Gibbs energies of the $TS_{(70)}$ and $TS_{(180)}$ points, respectively, estimated at 300 K.

Figure 3 shows the steps performed to improve the description of the energy profile for the chemiluminescence

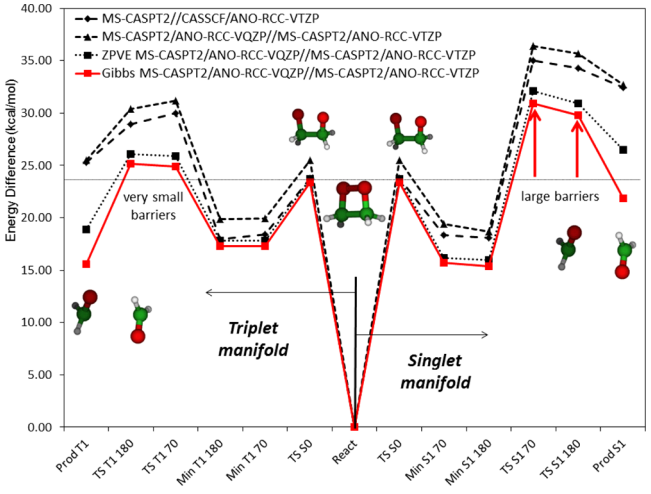

Figure 3. Relative energies of the stationary points obtained at different levels along the singlet and triplet manifolds. The energy barrier heights for the TS of the C−C bond dissociations ($TS_{S1(70)}$, $TS_{S1(180)}$, $TS_{T1(70)}$, and $TS_{T1(180)}$) are highlighted relative to the TS of the O−O bond breaking (TS_{S0}).

of 1,2-dioxetane with respect to the previous paper.[11] Whereas the improvements in the electronic energies, by means of the inclusion of dynamical correlation in the method for geometry optimization and the enlargement of the basis set, imply in general relatively small deviations, ZPVE corrections and the entropic factor change some aspects of the mechanism for chemiluminescence. The former results show TSs for the C−C′ bond cleavage higher in energy with respect to the TS related to the O−O′ bond breaking. This is true for both the singlet and triplet states and for the TSs with O−C−C′−O′ dihedral angles of 70° and 180°. Conversely, a more accurate description (including ZPVE and entropy corrections) brings the $TS_{T1(70)}$ and $TS_{T1(180)}$ structures close to the energy of the TS_{S0} point. In addition, taking into account the symmetry of the molecule, a total amount of two and six TS structures exist on the PESs related to the O−O′ and C−C′ bond dissociations, respectively, which will effectively reduce the activation barrier of the later process. This translates to that at 300 K the effective activation energies are 23.0, 23.9, and 29.2 kcal/mol for the O−O′ breakage on the S_0 surface, the C−C′ breakage on the T_1 surface, and the C−C′ breakage on the S_1 surface, respectively. Therefore, the rate-determining step for the phosphorescence emission is basically the O−O′ cleavage, and not the second C−C′ bond breaking as it is the case on the basis of the electronic energies.[11] The total energy needed to rupture the O−O′ bond seems to be enough to access the triplet TS and the emissive formaldehyde T_1 state. Fluorescence, on the other hand, still needs a significant amount of extra energy with respect to the level of the TS_{S0}, which makes the C−C′ bond dissociation more difficult and the emissive S_1 state less accessible. The phosphorescence process requires a population transfer from the ground state S_0 to the triplet state T_1. This is possible through the wide region of ISC crossing that exists between the TS_{S0} and the $TS_{T1(70)}$ or $TS_{T1(180)}$. The ISC is also probable because computations of the SOC give values as high as 49 cm^{-1} for the biradical structures (degeneracy region) of 1,2-dioxetane. A strict quantitative analysis of the ratio phosphorescence to fluorescence is subject to careful simulations including both internal conversion and interstate crossing. However, a preliminary rough estimation of the ratio based on the Arrhenius equation gives a value of $7903 \times (A_T/A_S)$, where A_T and A_S are the Arrhenius frequency factors for the triplet and single excited state dissociations. Considering that the second term (A_T/A_S) is smaller than unity, due to the fact that the single-triplet transition is forbidden to first order, the estimated ratio $(7903 \times (A_T/A_S))$ demonstrates that the presented activation energies of the triplet and singlet excited products are consistent with the observed ratio of phosphorescence to fluorescence. Also, the experimental threshold of 22.7 ± 0.8 kcal/mol[6] for chemiluminescence in 1,2-dioxetane is now rationalized by the fact that the triplet TSs related to the C−C′ cleavage are close in terms of energy to the TS_{S0}, in contrast to the previous study by De Vico et al.[11] This would make the activation of the ground state dissociation and the chemiluminescence from the phosphorescent triplet state literarily indistinguishable based on a study of the activation energy of the processes. This conclusion is in agreement with measurements for tetramethyldioxetane[9] and *cis*-diethoxy-1,2-dioxetane[10] and previous computed data with the CASSCF/MP2 method for the ground and lowest-lying triplet states.[8]

3.2. Two-Dimensional Model of the Decomposition Reaction. As explained in the Introduction, three types of mechanisms have been proposed for the chemiluminescence of 1,2-dioxetane: (1) concerted O−O′ and C−C′ bond dissociation, (2) two-step process involving a •O−CH_2−C′H_2−O• biradical intermediate, and (3) merged mechanism. The findings obtained by De Vico et al.[11] and the results from the previous section point to a biradical mechanism. In order to further verify it, we explore here the surroundings of the stationary points by means of the MS-CASPT2//CASSCF-(12in10)/ANO-RCC-VTZP method and a constraint geometry optimization procedure.

Even in such a small molecule as 1,2-dioxetane, the PES characterization by means of constraint optimizations must be performed with caution, comparing with additional data from strategies which provide accurate paths, such as MEPs and intrinsic reaction paths. In fact, our first attempt, selecting the C−C′ bond length and the O−C−C′−O′ dihedral angle as constraints, failed. From the reactant, the structure becomes "twisted" (see Figure 4) and does not connect it with the TS_{S0} structure as the MEP computations do (cf. De Vico et al.[11]). An

Figure 4. 1,2-Dioxetane structures obtained as TS in the constraint optimizations by two different sets of constraints: C−C′ bond length and O−C−C′−O′ dihedral angle (left) and C−C′ and O−O′ bond lengths (right).

dx.doi.org/10.1021/ct4007844 | J. Chem. Theory Comput. XXXX, XXX, XXX−XXX

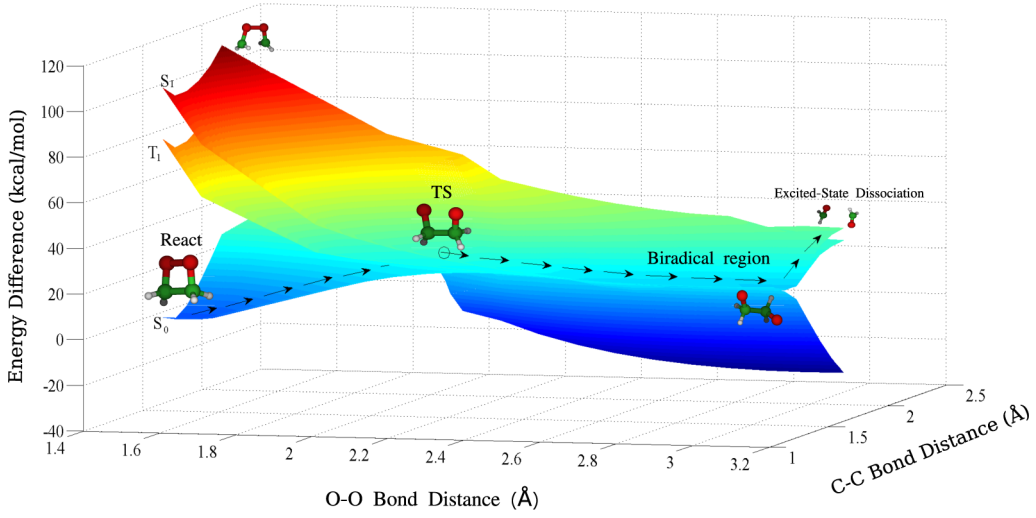

Figure 5. MS-CASPT2/ANO-RCC-VTZP energies (in kcal/mol) of the lowest-lying singlet and triplet excited states of 1,2-dioxetane vs the C−C′ and O−O′ bond lengths (in Å) for the CASSCF/ANO-RCC-VTZP constraint optimization of the singlet ground state, S_0.

appropriate set of constraints are the C−C′ and O−O′ bond distances, which reproduce the stationary points and MEPs. Figure 5 shows the two-dimensional PESs obtained in this manner for the singlet and triplet states. Taking into account the large barriers to reach the excited state and the absence of degeneracy in the C−C′ axis or the diagonal starting from the Reactant point in the PES, the concerted mechanism can be discarded. The most accessible path to the excited formaldehyde is clearly the initial formation of the biradical structure, which eventually must surmount the second barrier following a perpendicular direction to the one involved in the first process. Hence, these results also discard the merge mechanism in favor of the two-step biradical mechanism.

3.3. Lower-Bound Estimation for the Lifetime of the Biradical Intermediate. The formation of a •O−CH_2−C′H_2−O′• intermediate and the presence of an entropic trapping region in which the molecule can split the population among the lowest four singlet and four triplet states was proposed in the previous theoretical study by De Vico et al.[11] Our interest here is to estimate how fast can be the pass through the intermediate region before thermal decomposition by means of AIMD. We performed the trajectories on the S_0 PES without considering the transfer of population to the other states. This approximation will give us a lower-bound estimation, since the effect of CIX and ISC crossings among the degenerate states is expected to increase the time spent in this region.

A total amount of 300 trajectories were run at a constant T of 300 K from the TS_{S0} and using the CASSCF(6in6)/ANO-RCC-VDZP gradients of the ground state. All the dynamics computations give rise to the C−C′ dissociation within the limit time of 1 ps (see distribution of dissociation times in Figure 6). In agreement with the previous results obtained from the static modeling of the reaction, the dynamics simulations shows a torsion of the O−C−C′−O′ dihedral angle in the biradical region. MS-CASPT2(6in6)/ANO-RCC-VDZP calculations along the trajectories verify the degeneracy of the lowest four singlet and four triplet states, which disappears when the C−C′ bond breaks. The half-life time obtained as lower-bound for the entropic trap is 613 fs (to be compared with the oscillation time of a C−C′ single bond of about 30 fs). If the molecule has not on average transferred the population to the

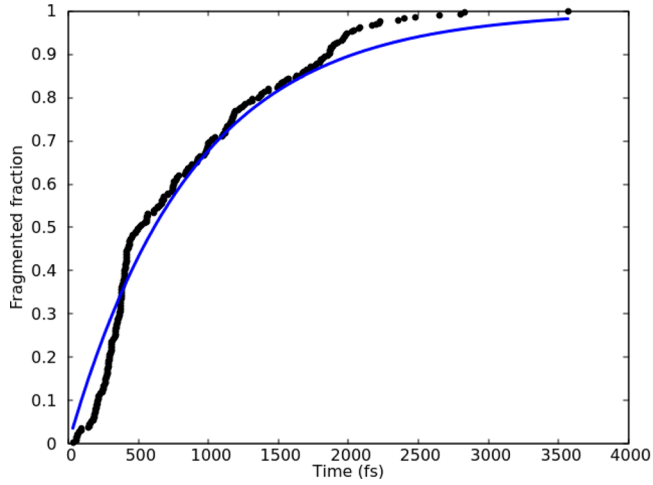

Figure 6. Fragmented fraction of the 300 trajectories (black dots) as a function of time in the ab initio molecular dynamics simulation in the canonical ensemble at 300 K. The blue line corresponds to an exponential decay with a half-life time of 613 fs. The simulation is conducted on the S_0 surface of 1,2-dioxetane after the TS_{S0} ignoring internal conversions and interstate crossings. The molecule is considered to be dissociated at a C−C′ bond distance larger than 2.3 Å.

excited singlet or triplet states after that time, it will decompose in the ground state without emission of light. According to the experimental data, the latter process, that is, the thermal dissociation, is the most probable process occurring in 1,2-dioxetane.[6] In order to produce fluorescence and phosphorescence, the system must reach the excited singlet and triplet states, respectively, along the biradical region. Crossings and recrossings among the four singlet and four triplet degenerate states, which are not considered in the current dynamics simulations, are expected to increase the lifetime of the entropic trap, thus explaining the luminescence properties. Further AIMD simulations considering nonadiabatic crossings between singlet states (CIX) and between singlet and triplet states (ISC) shall be performed in future works in order to provide quantitative quantum yields for the thermal dissociation,

dx.doi.org/10.1021/ct4007844 | J. Chem. Theory Comput. XXXX, XXX, XXX−XXX

fluorescence, and phosphorescence processes, to be directly compared with the experimental data.

We would like to point out that the dynamics presented here are in line with a non-RRKM behavior as demonstrated by Sun et al.[12] However, their study did not demonstrate an effect due to the entropic trapping and the formation of a biradical intermediate, rather the C−C′ bond rupture occurred at about 20 fs after the initial O−O′ bond rupture. This would correspond to the behavior of the few trajectories in this study which dissociate before 100 fs (see Figure 6). This difference between the results of the dynamics is possibly associated with (a) the underlying level of theory to describe the PES and (b) the starting structures of the respective molecular dynamics simulations. First, while we use MS-CASPT2 theory, Sun et al.[12] use unrestricted density functional theory; the latter puts the second TS at about 10 kcal/mol below the first TS, the former does not predict a clear TS at the C−C′ bond rupture but predicts a shoulder at around 2−3 kcal/mol below the first TS.[11] Effectively, the larger energy difference between the two TSs in the study by Sun et al. would amount to that no biradical intermediates are formed. Second, the simulations by Sun et al.[12] starts at a TS associated with the formation of dioxetane from molecular oxygen and ethene. This TS is about 45 kcal/mol above the energy of the dioxetane in its equilibrium structure. Hence, the molecule will, on the path toward the fragmentation to formaldehyde, reach the O−O′ bond rupture TS with an excess energy of about 20 kcal/mol. In this respect, a strong non-RRKM behavior is expected and the super hot species will not form a biradical intermediate.

4. CONCLUSIONS

The chemiluminescence reaction of 1,2-dioxetane is revisited in the present contribution. High-level CASSCF/CASPT2 calculations and AIMD simulations at T equal 300 K have been carried out in order to further understand the thermal dissociation and chemiluminescence processes of the molecule and to interpret some experimental observations which were still not accounted for, in particular, the high ratio of triplet to singlet dissociation products.

The findings confirm a stepwise mechanism for the chemiluminescence reaction, which can be described as follows. First, the O−O′ bond is broken and the molecule enters in an extended region of biradical character, in which four singlet and four triplet states are degenerated. Here, a biradical intermediate if formed which, in absence of internal conversion to the S_1 state and interstate crossing to the T_1 state, thermally dissociated wth a half-life time of 613 fs. The nonadiabatic process is possible in singlet as well as triplet states. A high probability for the spin-forbidden triplet population is predicted in this region, according to the SOC calculations. In order to produce chemiluminescence, a second energy barrier must be surmounted in the manifolds of the lowest-lying singlet or triplet excited states related to the C−C′ bond dissociation. This activation energy is lower in the triplet manifold, presenting a TS basically degenerated with the first TS on the ground state related to the O−O′ bond breaking, while the TS on the singlet excited state surface is about 6−7 kcal/mol higher in energy. Hence, in contrast to the fluorescence emission of light, the phosphorescence requires the same energy as the activation energy for the thermal dissociation (around 23−24 kcal/mol). These results are in agreement with the experiments and allow to rationalize the observed larger quantum yield of phosphorescence as compared to fluorescence.

■ ASSOCIATED CONTENT

Supporting Information

Cartesian coordinates and energies of the low-lying singlet and triplet states. This material is available free of charge via the Internet at http://pubs.acs.org.

■ AUTHOR INFORMATION

Corresponding Authors

*E-mail: Daniel.Roca@uv.es.
*E-mail: Roland.Lindh@kemi.uu.se.

Notes

The authors declare no competing financial interest.

■ ACKNOWLEDGMENTS

D.R.-S. thanks the Spanish MINECO source through project CTQ2010-14892. P.F. and R.L. acknowledge financial support from Behrouz Nik Ind and the Swedish Research Council (VR), respectively. The computations were performed on resources provided by SNIC through Uppsala Multidisciplinary Center for Advanced Computational Science (UPPMAX) under Project s00112-19.

■ REFERENCES

(1) Contag, C.; Bachmann, M. Advances in in vivo bioluminescence imaging of gene expression. *Annu. Rev. Biomed. Eng.* **2002**, *4*, 235.
(2) Jenkins, D.; Oei, Y.; Hornig, Y.; Yu, S.; Dusich, J.; Purchio, T.; Contag, P. Bioluminescence imaging (BLI) to improve and refine traditional murine models of tumor growth and metastasis. *Clin. Exp. Metastasis* **2003**, *20*, 733.
(3) Kopecky, K. R.; Mumford, C. Luminescence in the thermal decomposition of 3,3,4-trimethyl-1,2-dioxetane. *Can. J. Chem.* **1969**, *47*, 709−711.
(4) O'Neal, H. E.; Richardson, W. H. Thermochemistry of 1,2-dioxetane and its methylated derivatives. Estimate of activation parameters. *J. Am. Chem. Soc.* **1970**, *92*, 6553−6557.
(5) Turro, N. J.; Lechtken, P. Molecular photochemistry. LXII. Thermal generation of organic molecules in electronically excited states. Evidence for a spin forbidden, diabatic pericyclic reaction. *J. Am. Chem. Soc.* **1973**, *95*, 264−266.
(6) Adam, W.; Baader, W. J. Effects of methylation on the thermal stability and chemiluminescence properties of 1,2-dioxetanes. *J. Am. Chem. Soc.* **1985**, *107*, 410−416.
(7) Reguero, M.; Bernardi, F.; Bottoni, A.; Olivucci, M.; Robb, M. A. Chemiluminescent decomposition of 1,2-dioxetanes: an MC-SCF/MP2 study with VB analysis. *J. Am. Chem. Soc.* **1991**, *113*, 1566−1572.
(8) Wilsey, S.; Bernardi, F.; Olivucci, M.; Robb, M. A.; Murphy, S.; Adam, W. The thermal decomposition of 1,2-dioxetane revisited. *J. Phys. Chem. A* **1999**, *103*, 1669−1677.
(9) Steinmetzer, H.; Yekta, A.; Turro, N. J. Chemiluminescence of tetramethyl-1,2-dioxetane. Measurement of activation parameters and rates of exceedingly slow reactions by a simple and nondestructive method. Demonstration of indistinguishable activation energies for generation of acetone singlets and triplets. *J. Am. Chem. Soc.* **1974**, *96*, 282.
(10) Wilson, T.; Schaap, P. Chemiluminescence from cis-diethoxy-1,2-dioxetane. Unexpected effect of oxygen. *J. Am. Chem. Soc.* **1971**, *93*, 4126.
(11) De Vico, L.; Liu, Y.-J.; Krogh, J. W.; Lindh, R. Chemiluminescence of 1,2-dioxetane. reaction mechanism uncovered. *J. Phys. Chem. A* **2007**, *111*, 8013−8019.
(12) Sun, R.; Park, K.; de Jong, W.; Lischka, H.; Windus, T.; Hase, W. Direct dynamics simulation of the dioxetane formation and

decomposition via the singlet .O-O-CH2-CH2. biradical: Non-RRKM dynamics. *J. Chem. Phys.* **2012**, *137*, 044305.
(13) Roos, B. O.; Taylor, P. R.; Siegbahn, P. E. M. A complete active space SCF method (CASSCF) using a density matrix formulated super-CI approach. *Chem. Phys.* **1980**, *48*, 157−173.
(14) Roos, B. O. The complete active space SCF method in a Fock-matrix-based super-CI formulation. *Int. J. Quantum Chem.* **1980**, *S14*, 175−189.
(15) Andersson, K.; Malmqvist, P.-Å.; Roos, B. O.; Sadlej, A. J.; Wolinski, K. Second-order perturbation theory with a CASSCF reference function. *J. Phys. Chem.* **1990**, *94*, 5483−5488.
(16) Andersson, K.; Malmqvist, P.-Å.; Roos, B. O. Second-order perturbation theory with a complete active space self-consistent field reference function. *J. Chem. Phys.* **1992**, *96*, 1218−1226.
(17) Roca-Sanjuán, D.; Aquilante, F.; Lindh, R. Multiconfiguration second-order perturbation theory approach to strong electron correlation in chemistry and photochemistry. *Wiley Interdisciplinary Reviews: Computational Molecular Science* **2012**, *2*, 585−603.
(18) Roos, B. O.; Lindh, R.; Malmqvist, P.-Å.; Veryazov, V.; Widmark, P.-O. Main group atoms and dimers studied with a new relativistic ANO basis set. *J. Phys. Chem. A* **2004**, *108*, 2851−2858.
(19) Finley, J.; Malmqvist, P.-Å.; Roos, B.; Serrano-Andrés, L. The multi-state CASPT2 method. *Chem. Phys. Lett.* **1998**, *288*, 299−306.
(20) Serrano-Andrés, L.; Merchán, M.; Lindh, R. Computation of conical intersections by using perturbation techniques. *J. Chem. Phys.* **2005**, *122*, 104107.
(21) Ghigo, G.; Roos, B. O.; Malmqvist, P.-Å A modified definition of the zeroth-order Hamiltonian in multiconfigurational perturbation theory (CASPT2). *Chem. Phys. Lett.* **2004**, *396*, 142−149.
(22) De Vico, L.; Olivucci, M.; Lindh, R. New general tools for constrained geometry optimizations. *J. Chem. Theor. Comput.* **2005**, *1*, 1029−1037.
(23) Rubio-Pons, Ò.; Serrano-Andrés, L.; Merchán, M. A theoretical insight into the photophysics of acridine. *J. Phys. Chem. A* **2001**, *105*, 9664−9673.
(24) Strickler, S. J.; Berg, R. A. Relationship between absorption intensity and fluorescence lifetime of molecules. *J. Chem. Phys.* **1962**, *37*, 814.
(25) Aquilante, F.; De Vico, L.; Ferré, N.; Ghigo, G.; Malmqvist, P.-Å.; Neogrady, P.; Pedersen, T. B.; Pitonak, M.; Reiher, M.; Roos, B. O.; Serrano-Andrés, L.; Urban, M.; Veryazov, V.; Lindh, R. Software news and update MOLCAS 7: The next generation. *J. Comput. Chem.* **2010**, *31*, 224−247.
(26) Frenkel D., S. B. *Understanding Molecular Simulation*; Academic Press: San Diego, 2002.
(27) Tuckerman, M. E.; Martyna, G. J. Understanding modern molecular dynamics: Techniques and applications. *J. Phys. Chem. B* **2001**, *105*, 7598−7598.
(28) Martyna, G. J.; Tuckerman, M. E.; Tobias, D. J.; Klein, M. L. Explicit reversible integrators for extended systems dynamics. *Mol. Phys.* **1996**, *87*, 1117−1157.
(29) Field, M. *A Practical Introduction to the Simulation of Molecular Systems*; Cambridge University Press: New York, 2007; pp 1−344.
(30) Lourderaj, U.; Park, K.; Hase, W. L. Classical trajectory simulations of post-transition state dynamics. *Int. Rev. Phys. Chem.* **2008**, *27*, 361.
(31) Sun, L.; Park, K.; Song, K.; Setser, D. W.; Hase, W. L. Use of a single trajectory to study product energy partitioning in unimolecular dissociation: Mass effects for halogenated alkanes. *J. Chem. Phys.* **2006**, *124*, 064313.